Effect of carbon fiber type on monotonic and fatigue properties of orthopedic grade PEEK

Effect of carbon fiber type on monotonic and fatigue properties of orthopedic grade PEEK

Keywords: PEEK composites; fatigue crack propagation; orthopedic biomaterials; fractography

Noah Bonnheim, MS (corresponding author)
Department of Mechanical Engineering, University of California, Berkeley
2121 Etcheverry Hall
Berkeley, CA 94720
noah.bonnheim@berkeley.edu
(214) 288-1730
No conflicts of interest

Farzana Ansari, PhD
Exponent, Inc.
149 Commonwealth Drive
Menlo Park, CA 94025
No conflicts of interest

Marco Regis, PhD
Department of Chemistry, Università degli Studi di Torino
Via P. giuria 7
10125 Torino Italy
No conflicts of interest

Pierangiola Bracco, PhD
Department of Chemistry, Università degli Studi di Torino
Via P. giuria 7
10125 Torino Italy
No conflicts of interest

Lisa Pruitt, PhD
Department of Mechanical Engineering, University of California, Berkeley
2121 Etcheverry Hall
Berkeley, CA 94720
No conflicts of interest

Abstract

Carbon-fiber reinforced (CFR) PEEK implants are used in orthopedic applications ranging from fracture fixation plates to spinal fusion cages. Documented implant failures and increasing volume and variety of CFR PEEK implants warrant a clearer understanding of material behavior under monotonic and cyclic loading. To address this issue, we conducted monotonic and fatigue crack propagation (FCP) experiments on orthopedic grade unfilled PEEK and two formulations of CFR PEEK (PAN- and pitch-based carbon fibers). The effect of annealing on FCP behavior was also studied. Under monotonic loading, fiber type had a statistically significant effect on elastic modulus (12.5 ± 1.3 versus 18.5 ± 2.3 GPa, pitch versus PAN CFR PEEK, AVG ± SD) and on ultimate tensile strength (145 ± 9 versus 192 ± 17 MPa, pitch versus PAN CFR PEEK, AVG ± SD). Fiber type did not have a significant effect on failure strain. Under cyclic loading, PAN CFR PEEK demonstrated an increased resistance to FCP compared with unfilled and pitch CFR PEEK, and this improvement was enhanced following annealing. Pitch CFR PEEK exhibited similar FCP behavior to unfilled PEEK and neither material was substantially affected by annealing. The improvements in monotonic and FCP behavior of PAN CFR PEEK is attributed to a compound effect of inherent fiber properties, increased fiber number for an equivalent wt % reinforcement, and fiber aspect ratio. FCP was shown to proceed via cyclic modes during stable crack growth, which transitioned to static modes (more akin to monotonic fracture) at longer crack lengths. The mechanisms of fatigue crack propagation appear similar between carbon-fiber types.

1. Introduction

Poly(ether-ether-ketone) (PEEK) is a high-performance, biocompatible polymer which has been used in load-bearing orthopedic components since the 1990s [1]. The ability to formulate PEEK with fillers such as carbon fiber can result in mechanical properties suitable to a variety of orthopedic applications, including spinal fusion cages, fracture fixation plates, femoral stems, bone screws, intramedullary nails, and other devices [2].

The mechanical and thermal properties of PEEK are a function of its crystalline structure, chemical architecture, and morphology. PEEK is a semi-crystalline thermoplastic which, depending on processing, can be can be up to 43% crystalline [3], although 30-35% crystallinity is typical for PEEK used in medical devices [1,4,5]. The crystalline domains are generally lamellar in structure and can organize into spherulites [3,6]. Crystallinity can be controlled by altering the rate of cooling from the molten state during processing, or by using a post-processing thermal treatment such as annealing. Since molecular chains need time and energy to organize into crystalline domains, both slow cooling from the molten state and annealing enhance crystallinity in PEEK. Fillers such as carbon fiber also affect morphology by altering the geometry of crystalline domains as well as local cooling rates of the PEEK matrix [4,7–9].

The chemical backbone of PEEK is comprised of aromatic (benzene) units connected by ketone and ether groups. The monomer units form a linear homopolymer with approximately 100 units per chain and an average molecular weight of 80,000-120,000 g/mol [1]. While the molecule can rotate about the ether and ketone bonds, the large aromatic units inhibit chain mobility and require large amounts of thermal energy for bulk motion [1,4]. Accordingly, PEEK has a high glass transition temperature (145°C), a high melting temperature (340°C) [6] and is stable at the body's operating temperature of 37°C.

In addition to its thermal and mechanical properties, PEEK's radiolucency and radiative stability contribute to its orthopedic relevance. Metallic implants are radiopaque, inhibiting radiographic assessment of intra-implant bone formation by causing artefacts that can hinder clinical evaluation [10,11]. PEEK is radiolucent, enabling radiographic assessment using existing diagnostic imaging techniques [2]. In the spine, for example, radiographic evidence of bone density changes within a PEEK fusion cage can be used to assess the degree of fusion [12]. PEEK is stable when exposed to gamma radiation in doses relevant to implant sterilization (25-40 kGy) [2], and can also be sterilized using steam and ethylene oxide without appreciable degradation in mechanical properties [13].

The predominant clinical use of PEEK is in interbody fusion cages in the spine, where it is used in approximately 65% of the spinal fusion devices implanted annually in the U.S. [14]. PEEK has also shown promise in fracture fixation plates [15,16] and femoral stems [17,18]. Stress shielding in metallic fracture fixation plates [19] and hip stems [20] has motivated research into alternative structural materials, including PEEK. The use of carbon fiber to create a reinforced PEEK composite enables the modulus of some PEEK formulations to approximate, for example, cortical bone (approximately 17 GPa [21]), thereby theoretically reducing stress shielding. A number of carbon-fiber-reinforced (CFR) PEEK fracture fixation devices are now available and have shown promising clinical results [15,16]. PEEK as a femoral stem material has been the subject of much research and promising medium-term clinical results [22] but limited adoption in the U.S. While PEEK is used in only a fraction of the fracture fixation plates and hip stems implanted annually, its use is expected to rise with continued research and longer-term clinical data. This is especially relevant given the ongoing challenges with tissue modulus matching in orthopedic metals and the propensity for corrosion in metallic devices.

Unfilled and CFR PEEK have also been explored as bearing surfaces for total joint arthroplasty. *In vitro* tribological studies comparing the wear behavior of ultra-high-molecular-weight polyethylene (UHMWPE) with unfilled and CFR PEEK have shown mixed results [23–25]. Improvements in UHMWPE wear behavior, mixed PEEK data, and historical failures of CFR polymer bearing surfaces dating back to the 1970s may limit PEEK's use as a bearing material in the near-term. Nonetheless, new PEEK formulations are being developed and marketed as bearing surface alternatives [26].

CFR PEEK used in orthopedics commonly utilize one of two carbon-fiber types: PAN-based carbon fibers or pitch-based carbon fibers. PAN-based carbon fibers are derived from polyacrylonitrile and predominantly contain acrylonitrile monomer units, whereas pitch-based carbon fibers are typically derived from petroleum products and contain thousands of aromatic hydrocarbons [27,28]. The differences in carbon-fiber precursor requires different processing conditions and results in different fiber geometric and mechanical properties [27]. PAN-based carbon fibers can be stiffer, stronger, and are typically thinner than pitch-based carbon fibers (fiber elastic modulus 540 versus 280 GPa, fiber diameter 6 - 8 versus 10 - 20 μm, PAN versus pitch) [27,29,30]. The smaller diameter of PAN- compared to pitch-based carbon fibers as well as fiber density differences can result in more numerous fibers within a PAN CFR PEEK composite compared to a pitch CFR PEEK composite for an equivalent wt % reinforcement. Accordingly, PAN CFR PEEK composites can be stiffer and stronger than pitch-based counterparts [29]. Tribologically, PAN and pitch CFR PEEK exhibit similar wear rates, though these rates are sensitive to ambient temperature [27], dry versus lubricated articulation [25], conformity of contact [23], among other variables. Although tribological properties appear largely similar, pitch CFR PEEK is marketed as a material with beneficial tribological properties

(tradename PEEK-OPTIMA Wear Performance^{TM}) [26].

While not common, *in vivo* fractures of PEEK implants have been documented in the literature [31,32]. Additionally, *in vivo* fractures of other orthopedic devices comprising polymers (namely UHMWPE) and metals (namely cobalt-chromium, titanium, and stainless steel), have been documented extensively [33–35] and remain a limiting factor in clinical longevity. Despite the low prevalence of PEEK fractures, continually evolving material formulations and component designs warrant an understanding of the monotonic and fatigue fracture behavior of unfilled and pitch and PAN CFR PEEK.

A number of studies have explored effects of microstructural and processing variables on the fatigue and fracture behavior of PEEK [36–44]. In both unfilled and reinforced PEEK, matrix molecular weight can strongly influence fatigue crack propagation (FCP) resistance and the mechanisms of crack propagation [36,37,42]. An increase in molecular weight has been shown to improve resistance to FCP, an effect which has been partially attributed to an increased density of tie molecules connecting lamellar regions in higher molecular weight formulations, thereby strengthening the polymer matrix [36,37]. In unfilled PEEK, it has been shown that matrix molecular weight can precipitate differences in spherulite size, whereby spherulites will tend to grow larger in lower molecular weight PEEK [42]. Subsequently, crack growth tends to be intraspherulitic in lower molecular weight PEEK (i.e. through larger spherulites) and interspherulitic in higher molecular weight PEEK (i.e. around smaller spherulites) [42], reflecting fundamentally different mechanisms of crack propagation as a function of molecular weight. Enhanced crystallinity, which can be achieved via annealing [36,41,45], has also been shown to enhance resistance to FCP, though to a much lesser extent than molecular weight [36,37]. The mechanisms driving this improvement in FCP resistance are attributed to increased

energy required to deform and crack organized crystalline domains compared with amorphous domains [36,37]. Interestingly, while annealing increases the degree of crystallinity in unfilled and reinforced PEEK by similar amounts, improvements in FCP resistance induced by annealing have been shown to be greater in reinforced PEEK compared with unfilled PEEK [36]. It has been suggested that strong carbon fiber/PEEK matrix bonding produces crack initiation close to but not at the fiber/matrix interface (small amounts of matrix material may remain attached to the fibers), and thus FCP in short CFR PEEK is strongly dependent or even dominated by matrix properties, such as crystallinity, in regions close to the fibers [36]. The importance of the matrix properties in FCP in short CFR PEEK is supported by saturating improvements in FCP resistance with increasing fiber volume fraction [44]. While the addition of carbon fibers to a PEEK matrix introduces new energy dissipation mechanisms via fiber fracture and pullout, it also constrains the ability of the matrix to dissipate energy via plastic deformation [44]. Fiber fractions of 30% wt appear to offer little improvement in FCP resistance compared to volume fractions of 20% wt due to these competing energy dissipation mechanisms [44], thus underscoring the importance of matrix plasticity in FCP.

While previous studies have elucidated some microstructural and processing variables on the fatigue and fracture behavior of PEEK, there have been no studies directly comparing the FCP behavior of PAN versus pitch CFR PEEK. In light of documented *in vivo* fractures of orthopedic implants made of both polymeric and metallic components coupled with PAN and pitch CFR PEEK formulations designed specifically for orthopedic applications, it is the aim of the present investigation to describe the monotonic and FCP behavior of unfilled PEEK and pitch and PAN CFR PEEK. Additionally, the effect of annealing on FCP behavior is investigated. The materials studied were formulated specifically for use in orthopedic implants.

2. Methods

2.1 Material formulations

Three PEEK material formulations were studied:

(1) Unfilled PEEK (density 1.3 g/cm^3, tradename PEEK-OPTIMA^{TM} LT1, Invibio, Lankashire, UK)

(2) PAN CFR PEEK (density 1.3 g/cm^3, PEEK-OPTIMA^{TM} LT1 matrix with 30% wt PAN carbon fibers, tradename PEEK-OPTIMA Reinfored^{TM}, Invibio, Lankashire, UK). Fibers are short and randomly distributed (fiber modulus 540 GPa, fiber diameter 6 ± 2 μm, fiber length 230 ± 23 μm, fiber density 1.8 g/cm^3 [45])

(3) Pitch CFR PEEK (density 1.4 g/cm^3, PEEK-OPTIMA^{TM} LT1 matrix with 30% wt Pitch carbon fibers, tradename PEEK-OPTIMA Wear Performance^{TM}, Invibio, Lankashire, UK). Fibers are short and randomly distributed (fiber modulus 280 GPa, fiber diameter 10 ± 2 μm, fiber length 230 ± 13μm, fiber density 2.0 g/cm^3 [45])

Material granules were obtained from Invibio and processed into dog-bone and compact-tension (CT) specimens (Figure 1). Granules were first pre-heated to 70°C to remove residual moisture then injection molded into plates (250 x 25 x 2.5 mm). The injection nozzle temperature was held constant at 400°C and the mold at 250°C. Samples were cooled in air at room temperature. Water-jet machining was used to cut dog-bone and CT specimens from the plates, with the samples oriented for load application parallel to the mold-fill direction.

Three heat treatments were examined to investigate the effects of post-processing thermal treatment on FCP behavior. Samples were either non-annealed, annealed at 200°C, or annealed at 300°C. Annealing was conducted for five hours in a Nabertherm oven (Lilienthal, Germany),

159 with an initial heating rate of 5°C/min. After annealing, samples were cooled in air at room
160 temperature. Annealing was performed by Lima Corporate (Udine, Italy).

161 ***2.2 Monotonic testing***

162 Tensile testing to failure was performed on non-heat-treated samples in accordance with
163 ASTM D638 on type V dog-bone specimens (n=4 samples tested per material for a total of 12
164 tests). Monotonic mechanical testing for equivalent heat-treated materials has been reported
165 elsewhere [25,46] and was therefore not repeated here. Displacement was applied at a rate of 0.5
166 mm/min in ambient conditions (21°C / 28% RH) using a screw-driven Instron (model 5500R).
167 Strain was measured using a video extensometer (Instron, model 2663-821). Temperature of the
168 gauge-section was not measured during monotonic testing. Due the viscoelastic nature of
169 thermoplastic polymers, reported mechanical properties should be understood within the context
170 of displacement rate and ambient temperature. However, it has been previously shown that at
171 room temperature (≈ 124 °C below PEEK's glass transition temperature), varying displacement
172 rate by over four orders of magnitude (from 0.05 to 50 mm/min) had little effect on elastic
173 modulus and increased yield stress by less than 1.4x [47].

174 Elastic modulus (E), ultimate tensile strength (σ_{ut}), and elongation at failure (ε_f) were
175 reported for each material. Elastic modulus was calculated using a secant approximation
176 between 0.1% and 0.5% strain for each specimen. Student's t-tests were used to compare E, σ_{ut},
177 and ε_f between material formulations with significance assumed at $p \leq 0.05$.

178 ***2.3 Fatigue testing***

179 Fatigue crack propagation (FCP) experiments were conducted on CT specimens using a
180 servo-hydraulic Instron (model 8871) and a load-controlled sinusoidal wave function at a
181 frequency of 5 Hz [41,43]. Testing was performed at room-temperature and an air-cooling

system was used to minimize hysteretic heating [48]. The load ratio (minimum load/maximum load) was held constant at 0.1. A pre-crack of 1 mm was introduced at the tip of each notch using a razor blade and custom fixture, and datum dots were placed on specimen sides for subsequent image analysis [48]. Crack length was measured using a variable magnification optical system (Infinivar CFM-2/S, 5μm/pixel) and a digital video camera (Sony XCD-SX910). A custom LabView program controlled the camera, which captured images every 500 or 1000 cycles, depending on crack velocity. Custom scripts were created in ImageJ and MATLAB to semi-automate data analysis. A minimum of three samples were tested for each material formulation. The Paris equation (Equation 1) was used to map FCP as a function of cyclic stress intensity, where da/dN is the rate of crack velocity (mm/cycle), ΔK is the cyclic stress intensity (i.e. the crack driving force, MPa√m), and C (pre-exponent) and m (exponent, slope on logarithmic scale) are material constants. Any data not meeting the condition of small scale yielding (Equation 2) were excluded from this analysis, where (W-a) is the uncracked ligament length, K_{max} is the maximum mode-one stress intensity (MPa√m), and σ_{ys} is the material yield strength (MPa).

$$\frac{da}{dN} = C\Delta K^{m} \qquad \text{Equation 1}$$

$$(W - a) \geq \frac{4}{\pi}\left(\frac{K_{max}}{\sigma_{ys}}\right)^{2} \qquad \text{Equation 2}$$

2.4 Fractography

Fracture surfaces were imaged with scanning electron microscopy (SEM, Quanta FEI and Versa 3D Dual Beam) at 50-500x and optical microscopy (Keyence VHX 6000) at 10-50x. Some specimens were sputter coated in gold-vanadium to facilitate fracture surface visualization.

3. Results

3.1 Monotonic testing results

Compared with pitch CFR PEEK, PAN CFR PEEK exhibited a significantly higher elastic modulus (18.5 ± 1.3 vs 12.5 ± 1.3 GPa, PAN vs pitch CFR PEEK, $p = 0.006$, AVG ± SD) and ultimate tensile strength (192 ± 17 vs 145 ± 9 MPa, PAN vs pitch CFR PEEK, $p = 0.005$, AVG ± SD) (Table 1). Strain at failure was not significantly different between fiber types (1.9 ± 0.2 vs 2.2 ± 0.2 % strain, PAN vs pitch CFR PEEK, $p = 0.116$, AVG ± SD) (Table 1). Unfilled PEEK had a significantly lower elastic modulus (3.9 ± 0.2 GPa, AVG ± SD) and ultimate tensile strength (93 ± 1 MPa), and a significantly higher strain at failure (66 ± 7 %, AVG ± SD) compared with either fiber type ($p \leq 0.002$) (Table 1). In terms of the stress-strain behavior, unfilled PEEK demonstrated appreciable post-yield deformation (necking), whereas both pitch and PAN CFR PEEK failed in a predominantly brittle manner, at low failure strains and with little post-yield deformation (Figure 2).

3.2 Fatigue testing results

The crack velocity (da/dN) versus cyclic stress intensity (ΔK) curves for all PEEK materials generally followed a linear relationship in log-log space as described by the Paris Law (Equation 1, Figure 3). The region of stable crack growth was measured as $3.2 \leq \Delta K \leq 7.1$ MPa√m for unfilled PEEK, $4.2 \leq \Delta K \leq 6.8$ MPa√m for pitch CFR PEEK, and $4.6 \leq \Delta K \leq 8.6$ MPa√m for PAN CFR PEEK (all heat treatments). A rightward shift was observed in the PAN CFR PEEK data compared with the pitch CFR and unfilled PEEK data (all heat treatments). This rightward shift suggests an improvement in FCP resistance—a larger cyclic stress intensity was required to propagate a crack at a given velocity. The effect of annealing on FCP behavior appears small for unfilled and pitch CFR PEEK, evidenced by largely overlapping da/dN versus ΔK data (Figure 3). Annealing at 300 °C appears to have a more pronounced effect for PAN

CFR PEEK, evidenced by the distinct da/dN versus ΔK data between PAN and PAN 300 (Figure 3).

To clarify and quantify these observations, least squares regression analysis was used to generate best fit lines of the data (Figure 4). ΔK values at a constant crack velocity of da/dN = 2×10^{-4} mm/cycle were compared in order to quantify the relative resistance to FCP as well as the effect of annealing at an intermediate crack velocity (Table 2). The value of da/dN = 2×10^{-4} mm/cycle was chosen because it represents a crack velocity approximately centered within the linear (Paris) growth regime, approximately halfway between near-threshold and near fast-fracture regions based on the spread of the measured data (Figure 3, Figure 4). For non-annealed formulations, propagating a crack at da/dN = 2×10^{-4} mm/cycle required ΔK =4.9 MPa√m for unfilled PEEK, ΔK = 4.7 MPa√m for pitch CFR PEEK, and ΔK = 5.7 MPa√m for PAN CFR PEEK (Table 2). Thus, non-annealed unfilled and pitch CFR PEEK require a similar ΔK for intermediate crack velocities while non-annealed PAN CFR PEEK requires an increased ΔK on the order of 17-21% compared with unfilled and pitch CFR PEEK, respectively. For formulations annealed at 300 °C, the ΔK values required to propagate a crack at da/dN = 2×10^{-4} mm/cycle remain similar between unfilled and pitch CFR PEEK (4.7 versus 4.8 MPa√m, respectively) but increased to 7.0 MPa√m for PAN CFR PEEK, representing an increase of 45-50%.

The effect of heat-treatment on FCP resistance was thus relatively minor for unfilled PEEK, with a maximum ΔK variation of 0.3 MPa√m (6%) amongst heat treatments at da/dN = 2×10^{-4} mm/cycle. Similarly, the effect of heat treatment was relatively minor for pitch CFR PEEK, with a maximum ΔK variation of 0.5 MPa√m (9%) amongst heat treatments at da/dN = 2×10^{-4} mm/cycle. Conversely, heat-treatment had a larger effect on PAN CFR PEEK, with a

maximum ΔK variation of 1.5 MPa$\sqrt{m}$ (24%) amongst heat treatments at $da/dN = 2 \times 10^{-4}$ mm/cycle.

The linear regression analysis also enabled calculation of the Paris exponent (m in Equation 1), a material-specific parameter describing the rate of crack acceleration. Larger values of m indicate larger rates of crack accelerations. Values of m ranged between 4 - 5.1 for unfilled PEEK, 6.6 – 8.0 for pitch CFR PEEK, and 5.9 – 6.3 for PAN CFR PEEK (Figure 5). Thus, we observe a trend towards larger values of crack acceleration for both pitch and PAN CFR PEEK compared with unfilled PEEK, suggesting that the addition of carbon-fibers can increase the rate of crack acceleration. Heat-treatment appeared to have a minor and non-constant effect on m (Figure 5). In unfilled and pitch CFR PEEK, annealing decreased m, whereas for PAN CFR PEEK, annealing at 200 °C and 300 °C resulted in an increase in m of 17% and 7%, respectively (6.9 and 6.3 versus 5.9).

3.3 Fractography

Under monotonic loading, the fracture surface of unfilled PEEK displayed macroscopic plastic deformation including tearing features and a reduced cross-sectional area at the location of fracture (a result of necking) (Figure 6). The fracture surfaces of pitch and PAN CFR PEEK were similar to each other, displaying little bulk plastic deformation in comparison with unfilled PEEK (Figure 6). Pitch and PAN CFR PEEK display fiber fracture and fiber pull-out throughout the fracture surface (Figure 6).

Under fatigue loading, unfilled PEEK exhibited striation-like markings and parabolic features in the stable growth regime (Figure 7). The parabolic features tended to grow larger at longer crack lengths (Figure 7E). Compared with the stable growth region, the unstable growth

region in unfilled PEEK exhibited much greater amounts of plastic deformation, evidenced by localized contraction (necking) around the crack tip (Figure 7A).

Pitch and PAN CFR PEEK present with little macroscopic deformation (Figure 8), resulting from suppression of plastic deformation due to the presence of carbon fibers. During stable FCP, some fiber fracture and pull-out were observed in combination with near-tip local deformation of the matrix material (Figure 8B, 8E). During unstable FCP, these local matrix deformation features are not observed and the fracture surfaces instead display primarily fiber fracture and fiber pull-out (Figure 8C, 8F).

There were no observable fractographic distinctions in macroscopic (reinforcement-level) failure mode or mechanism between heat-treatments for unfilled PEEK and pitch and PAN CFR PEEK. Higher imaging magnifications may illuminate crystalline-level mechanisms and warrants further investigation.

4. Discussion

It was the aim of the current study was to investigate the effects of PAN- and pitch-based carbon fibers on the monotonic properties and FCP resistance of orthopedic grade PEEK. Additionally, we sought to elucidate the effects of annealing on FCP resistance.

Complete crystallinity data for the materials used in this study have been reported elsewhere [25]. Briefly, crystallinity for non-annealed PEEK is ≈ 32%, and all non-annealed formulations (i.e. unfilled, pitch and PAN CFR PEEK) are within 1% of this value [25]. Annealing enhances crystallinity in unfilled and pitch and PAN CFR PEEK by similar amounts: Low temperature (200 °C) annealing enhances crystallinity by ≈ 1% while high temperature (300 °C) annealing enhances crystallinity by ≈ 9% [25].

294 The addition of both pitch and PAN carbon fibers to the PEEK matrix increased
295 monotonic stiffness and strength and decreased ductility (strain to failure) compared with
296 unfilled PEEK. These trends are consistent with data published by the material manufacturer
297 [26,49,50] and with the behavior of many short-fiber thermoplastic polymer composites.
298 Comparing fiber types, we observed statistically significant increases of 48% in elastic modulus
299 and 32% in ultimate tensile strength, and a non-statistically significant decrease of 14% in strain
300 to failure for PAN versus pitch CFR PEEK. Increases in elastic modulus and ultimate tensile are
301 attributed to a number of microstructural characteristics, including inherent fiber mechanical
302 properties, differences in fiber number, and differences in fiber aspect ratio. The PAN-based
303 carbon fibers used in this study are 93% stiffer than pitch-based carbon fibers (elastic modulus
304 540 versus 280 GPa, PAN- versus pitch-based carbon fibers, respectively) [29]. Thus, composite
305 mechanical property differences would be expected even if other parameters (fiber number, fiber
306 aspect ratio, interfacial bonding, crystallinity, etc.) were equivalent. Further, PAN-based carbon
307 fibers are thinner and less dense than pitch-based carbon fibers (diameter 6 versus 10 μm,
308 density 1.8 versus 2.0 g/cm^3, PAN- versus pitch-based carbon fibers, respectively), and we thus
309 expect ≈3.1 times more PAN-based carbon fibers in a given specimen compared with pitch-
310 based carbon fibers for an equivalent wt % reinforcement (both composites used in this study
311 contained 30% wt fiber reinforcement). In a related vein, since the diameter of PAN-based
312 carbon fibers are smaller than pitch-based carbon fibers, the ratio of fiber surface area to fiber
313 volume will be enhanced in PAN versus pitch CFR PEEK for an equivalent fiber volume
314 fraction, thereby providing more surface area for the PEEK matrix to bond to PAN-based carbon
315 fibers. We suggest that improvements in mechanical behavior for PAN versus pitch CFR PEEK
316 are attributed to these compound effects: PAN-based carbon fibers are themselves stiffer, more

317 PAN-based carbon fibers are present, and comparatively more PAN-based carbon fiber surface
318 area is exposed to PEEK matrix, thus enhancing the area available for fiber/matrix bonding.
319 Under fatigue loading, we found that the addition of pitch-based carbon fibers did not
320 enhance FCP resistance, as the da/dN versus ΔK behavior for unfilled and pitch CFR PEEK are
321 similar. FCP resistance of these materials was largely unaffected by either low-temperature (200
322 °C) or high-temperature (300 °C) annealing. Conversely, the FCP resistance of PAN CFR PEEK
323 was appreciably improved compared with unfilled and pitch CFR PEEK. For non and low-
324 temperature annealed PAN CFR PEEK, the improvement was on the order of 17-21%, while for
325 high-temperature annealed PAN CFR PEEK the improvement was on the order of 45-50% at an
326 intermediate crack velocity.
327 The complex interdependence of microstructural parameters including manufacturing-
328 and annealing-induced matrix crystallinity, fiber type, fiber number, and fiber aspect ratio,
329 coupled with complex dynamics of FCP in polymer composites, make it difficult to
330 unambiguously differentiate individual microstructural effects on FCP behavior. Yet, a number
331 of observations warrant discussion.
332 The addition of fibers to a polymer matrix can enhance resistance to FCP by introducing
333 energy dissipation mechanisms via fiber fracture and pull-out [44]. Simultaneously, fibers can
334 inhibit energy dissipation by limiting the ability of the matrix to deform plastically [44]. The
335 balance between net energy dissipation/absorption (thus FCP improvement/degradation) depends
336 on a balance between matrix ductility (which depends on matrix molecular weight, crystallinity,
337 etc.), fiber properties, and the properties of the fiber/matrix interface. Previous studies have
338 shown that the addition of 30% wt. randomly distributed short glass fibers to a PEEK matrix
339 provided little to no improvement in FCP resistance, while the addition of 30% wt. randomly

distributed carbon fibers provided at least some improvement in FCP resistance [36,41,43] (the carbon fiber type is not mentioned in these studies, however PAN-based carbon fibers are the likely historical precedent [51]). This phenomenon is attributed to stronger fiber/matrix adhesion between the carbon fibers and the PEEK matrix compared with glass fibers and the PEEK matrix [36,41,44]. The results found in the current study, in which the addition of pitch-based carbon fibers provided little to no improvement in FCP resistance, while the addition of PAN-based carbon fibers provided an appreciable improvement in FCP resistance, could be plausibly explained via the same mechanism; stronger fiber/matrix adhesion in PAN- compared with pitch-based PEEK composites. However, aforementioned differences in inherent fiber properties, fiber numbers, and fiber aspect ratios confound and preclude a definitive statement on interfacial bond strength. Indeed, the fact that observed improvements in FCP resistance for PAN CFR PEEK are not commensurate with the magnitude of differences in fiber properties or fiber number could plausibly suggest a weaker interfacial bond for PAN versus pitch CFR PEEK. Additional studies are required to clarify differences in interfacial bond strength, which could be achieved via FCP tests controlling for fiber aspect ratio and/or fiber number.

Annealing has been shown to have a greater impact on FCP resistance for CFR PEEK compared with unfilled PEEK (carbon fiber type not specified), even when similar overall increases in crystallinity are induced by annealing [36,41]. Results found in the current study for PAN CFR PEEK are similar—annealing had no measurable effect on unfilled PEEK but appreciably improved FCP resistance in PAN CFR PEEK. It has been suggested that annealing may preferentially influence the matrix in regions near the fiber/matrix interface [36]. Thus, while it is not clear why annealing had no measurable effect on pitch CFR PEEK, one plausible explanation is that a lower fiber number in pitch versus PAN CFR PEEK (thus fewer

363 fiber/matrix interfacial regions) makes any preferential improvements in crystallinity less
364 pronounced. It has also been suggested that annealing enhances crystalline growth of the PEEK
365 matrix onto the carbon fiber surface, thereby improving interfacial bond strength [41]. Thus, a
366 second and related explanation follows that differences in crystallization mechanisms between
367 PAN and pitch CFR PEEK [45] contribute to differences in interfacial bond strength as a
368 function of annealing, even for similar overall degrees of crystallinity.

369 Fractographic analysis of failure surfaces suggest two distinct modes of FCP in PEEK,
370 notably a cyclic mode acting at low crack growth rates and a static mode acting at high crack
371 growth rates, as described by previous studies [37,38,40,43,44].

372 In unfilled PEEK, the stable growth regime exhibited striation-like markings (Figure 7B,
373 7C), similar to those reported previously [37,38,40,41,44], presumably caused by crack blunting
374 and re-sharpening during cyclic loading. The average width of the striation-like bands were not
375 measured in this study and compared to da/dN to confirm whether they were true fatigue
376 striations. Yet, previous investigations [37,40,41] confirmed markings of similar size and
377 morphology to be true fatigue striations. The observed parabolic features (Figure 7C, 7E) are
378 also consistent with previous investigations [37,41,44], and are attributed to the intersection of
379 the primary crack front with secondary cracks induced by inherent flaws. Unlike the stable
380 growth regime, the fast-fracture regime in unfilled PEEK is characterized by ductile contraction
381 (i.e. necking) in the zone around the crack tip. This ductile contraction in fast fracture region is
382 not apparent during stable crack growth but is apparent for monotonically tested PEEK.

383 Failure surfaces of pitch and PAN CFR PEEK also show evidence of an interaction
384 between cyclic and static mechanisms during FCP in line with previous studies on CFR PEEK
385 [44]. At low crack growth rates, we observe regions of matrix deformation and rupture near to

and along the fiber/matrix interface, as well as fiber fracture and pull-out (Figure 8B, 8E). It has been previously shown that under cyclic loading, local failure is dominated by separation along the fiber/matrix interfaces and rupture of the matrix material between fibers [36,43]. At higher crack growth rates, equivalent matrix deformation is not observed, and the fracture surface is instead comprised primarily of fiber fracture and pull-out (Figure 8C, 8F) more akin to monotonically tested samples (Figure 6). Thus, our findings offer supporting evidence for cyclic modes of growth at low growth rates which transition to static modes near the onset of failure in unfilled and both pitch and PAN CFR PEEK.

While the CFR PEEK formulations used in this study were reinforced using short, randomly distributed fibers to achieve bulk isotropy, the injection molding process has been shown to introduce some fiber alignment in proximity to the specimen surface (i.e. a "skin" layer) induced by friction with the mold wall [29,36,41,43,44]. This well-documented skin-core structure has been shown to produce more rapid crack growth when load is applied perpendicular to the mold-fill direction (thus crack growth parallel to the mold-fill direction) compared with the converse orientation [43,44]. Thus, the results here are limited to load application parallel to the mold fill direction.

5. Conclusion

Under monotonic loading, PAN CFR PEEK exhibited a larger elastic modulus and ultimate tensile strength compared with unfilled and pitch CFR PEEK. Under cyclic loading, PAN CFR PEEK exhibited an improved resistance to fatigue crack propagation compared with unfilled and pitch CFR PEEK. The improvement in fatigue crack propagation resistance for PAN CFR PEEK was enhanced following high-temperature (300 °C) annealing.

Pitch CFR PEEK did not exhibit improved fatigue crack propagation resistance compared with unfilled PEEK. Neither low temperature (200 °C) nor high temperature (300 °C) annealing produced a measurable effect on the fatigue crack propagation behavior of these materials.

The improvement in mechanical properties for PAN CFR PEEK is attributed to a compound affect: PAN-based carbon fibers are themselves stiffer than pitch-based carbon fibers, more PAN-based carbon fibers are present compared with pitch-based carbon fibers for an equivalent wt % reinforcement, and comparatively more PAN-based carbon fiber surface area is exposed to PEEK matrix, thus enhancing the area available for fiber/matrix bonding. Differences in fiber/matrix interfacial bond strength between PAN- versus pitch-based carbon fibers should be further elucidated, possibly via studies controlling for fiber number and/or aspect ratio.

Fatigue crack propagation was shown to proceed via cyclic modes during stable crack growth, characterized by striation-like bands and parabolic features in unfilled PEEK and matrix rupture near to and along the fiber/matrix interface in pitch and PAN CFR PEEK. Cyclic modes transition to static modes (more akin to monotonic fracture) at longer crack lengths, characterized by necking in unfilled PEEK and an increased degree of fiber fracture and pull-out in pitch and PAN CFR PEEK. The mechanisms of fatigue crack propagation appear similar between carbon-fiber types.

6. Figures and Tables

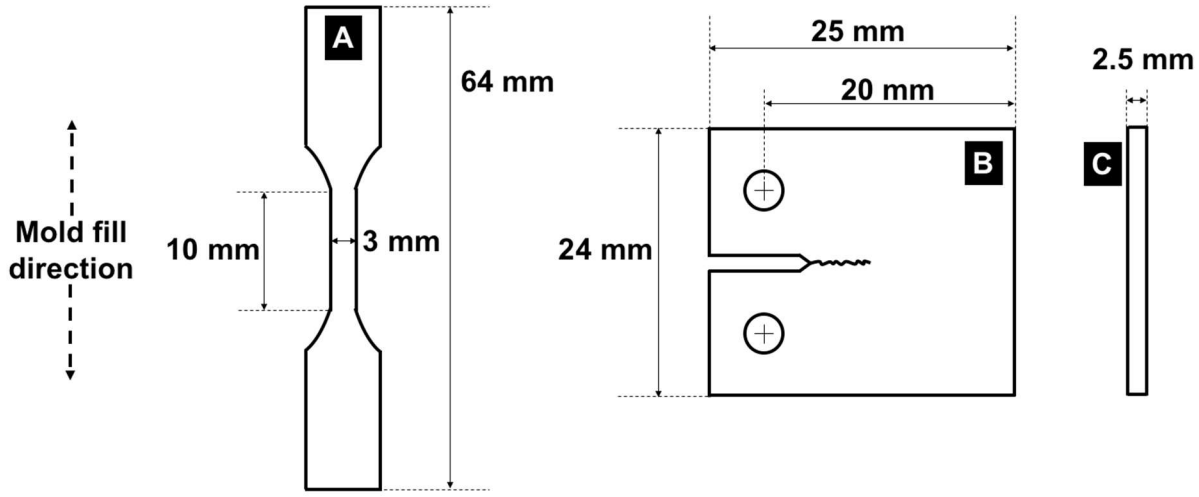

Figure 1. A) ASTM D638 type V dog-bone specimens used for monotonic testing. B) Compact-tension (CT) specimen used for FCP testing. C) Thickness for all specimens. Samples were oriented for load application parallel to the mold fill direction. Drawings are not to scale.

Table 1. Material properties for PEEK materials (non-heat-treated formulations).

	Unfilled	Pitch	PAN
E (GPa)	3.9 ± 0.2	12.5 ± 1.3	18.5 ± 2.3
σ_{ut} (MPa)	93 ± 1	145 ± 9	192 ± 17
ε_f (%)	66 ± 7	2.2 ± 0.2	1.9 ± 0.2

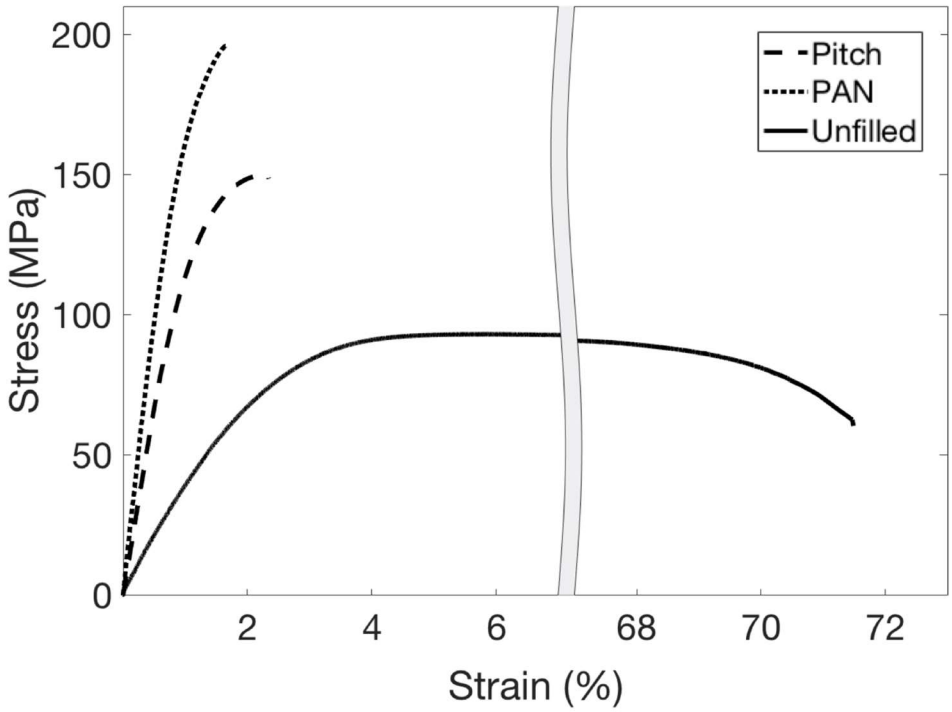

Figure 2. Representative stress-strain plots for Pitch CFR PEEK, PAN CFR PEEK, and unfilled PEEK (non heat-treated formulations).

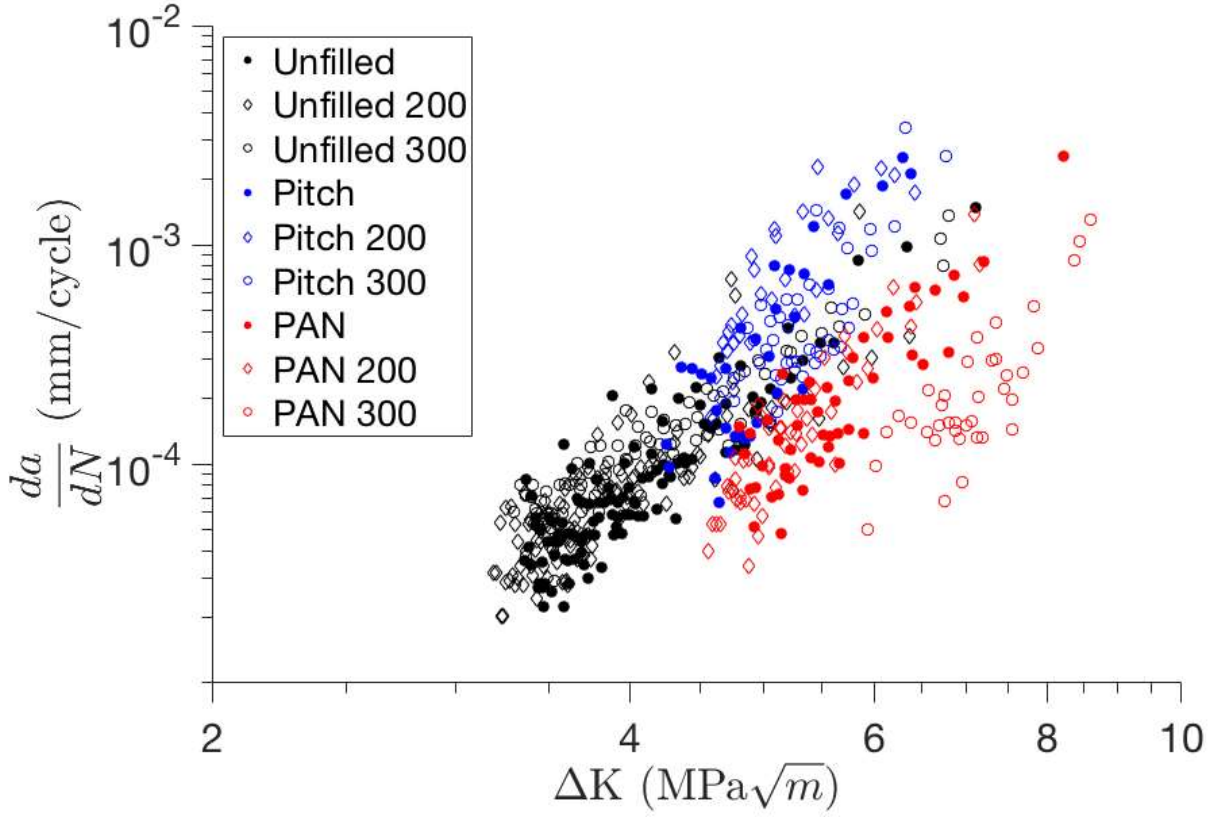

Figure 3. FCP plots for all material formulations and heat-treatments.

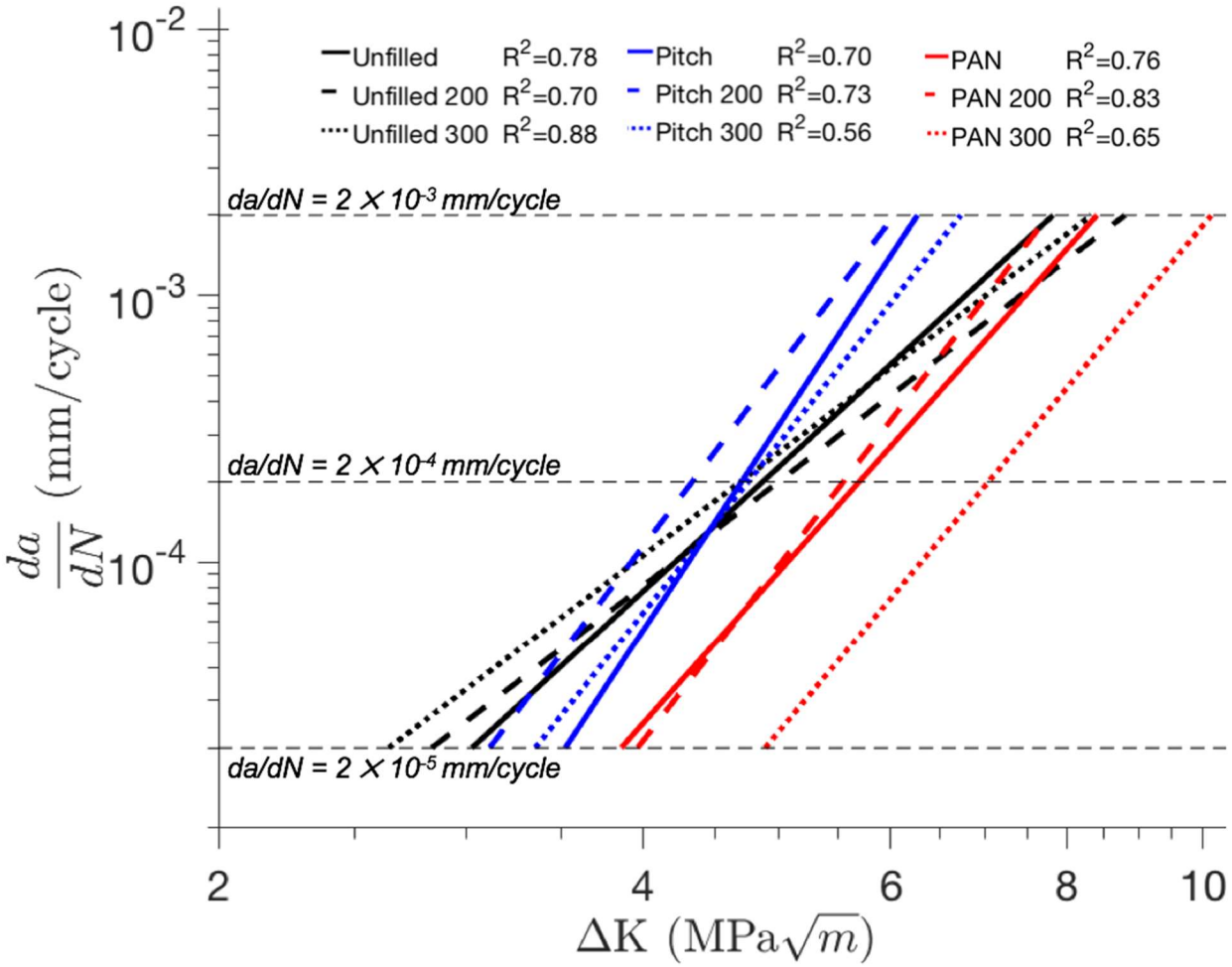

Figure 4. Paris fits for all materials. A constant crack velocity of da/dN = 2 × 10^{-4} mm/cycle was chosen to represent an intermediate crack velocity.

Table 2. ΔK values at the intermediate crack velocity of da/dN = 2×10^{-4} mm/cycle for all materials.

	ΔK (MPa√m) at da/dN = 2×10^{-4} mm/cycle
Unfilled	
0 °C	4.9
200 °C	5.0
300 °C	4.7
Pitch	
0 °C	4.7
200 °C	4.3
300 °C	4.8
PAN	
0 °C	5.7
200 °C	5.6
300 °C	7.0

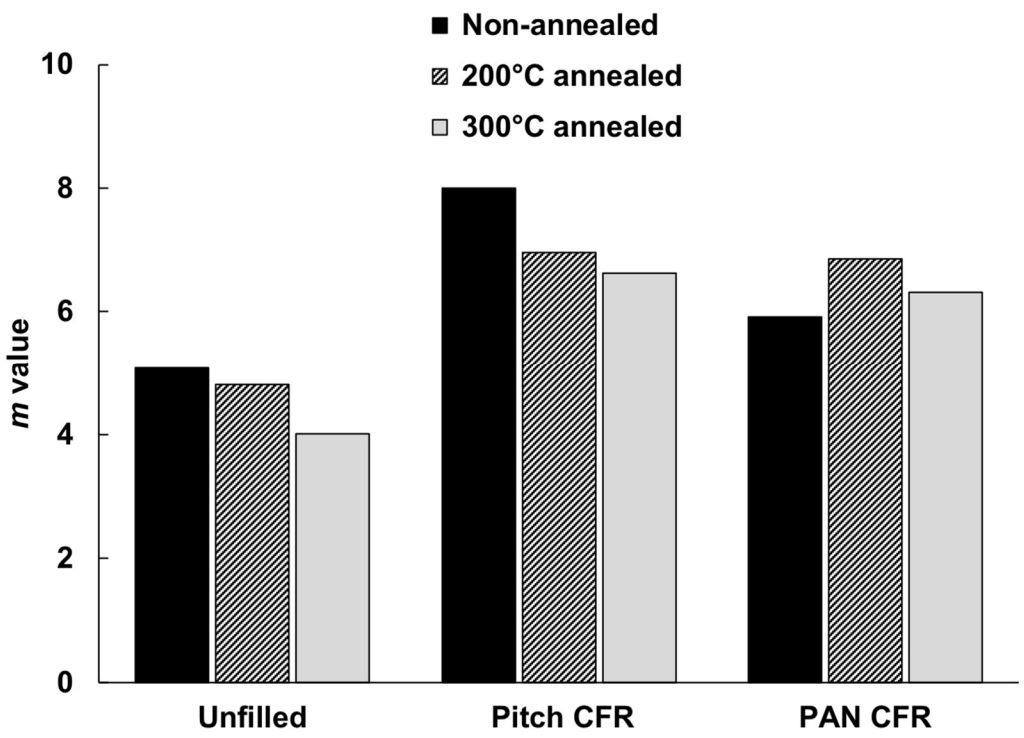

Figure 5. Paris constant, m, describing the rate of crack acceleration (slope of the da/dN versus ΔK plot) for all material formulations and heat-treatments.

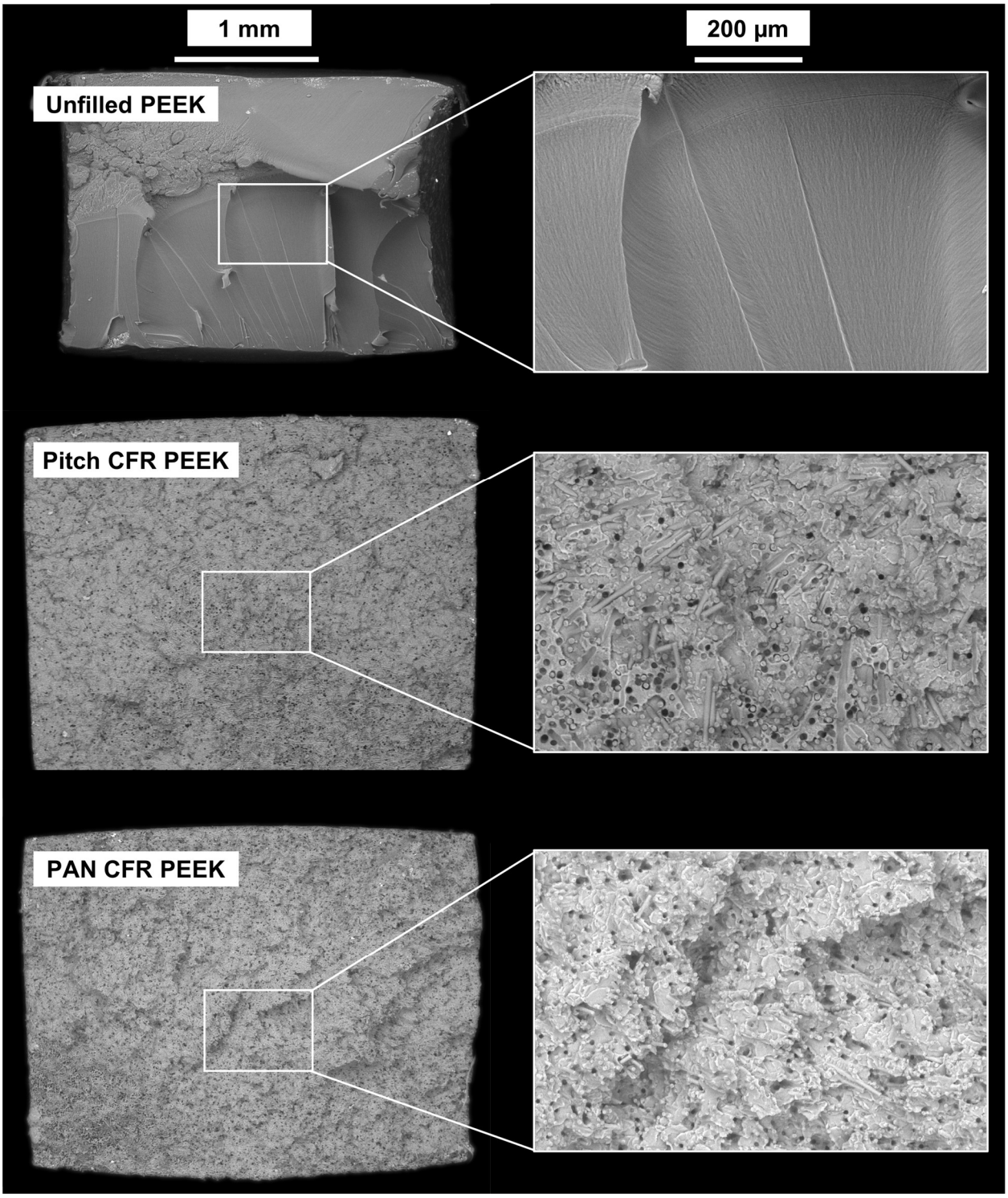

Figure 6. SEM images of the fracture surfaces of monotonically tested samples (non-heat-treated formulations).

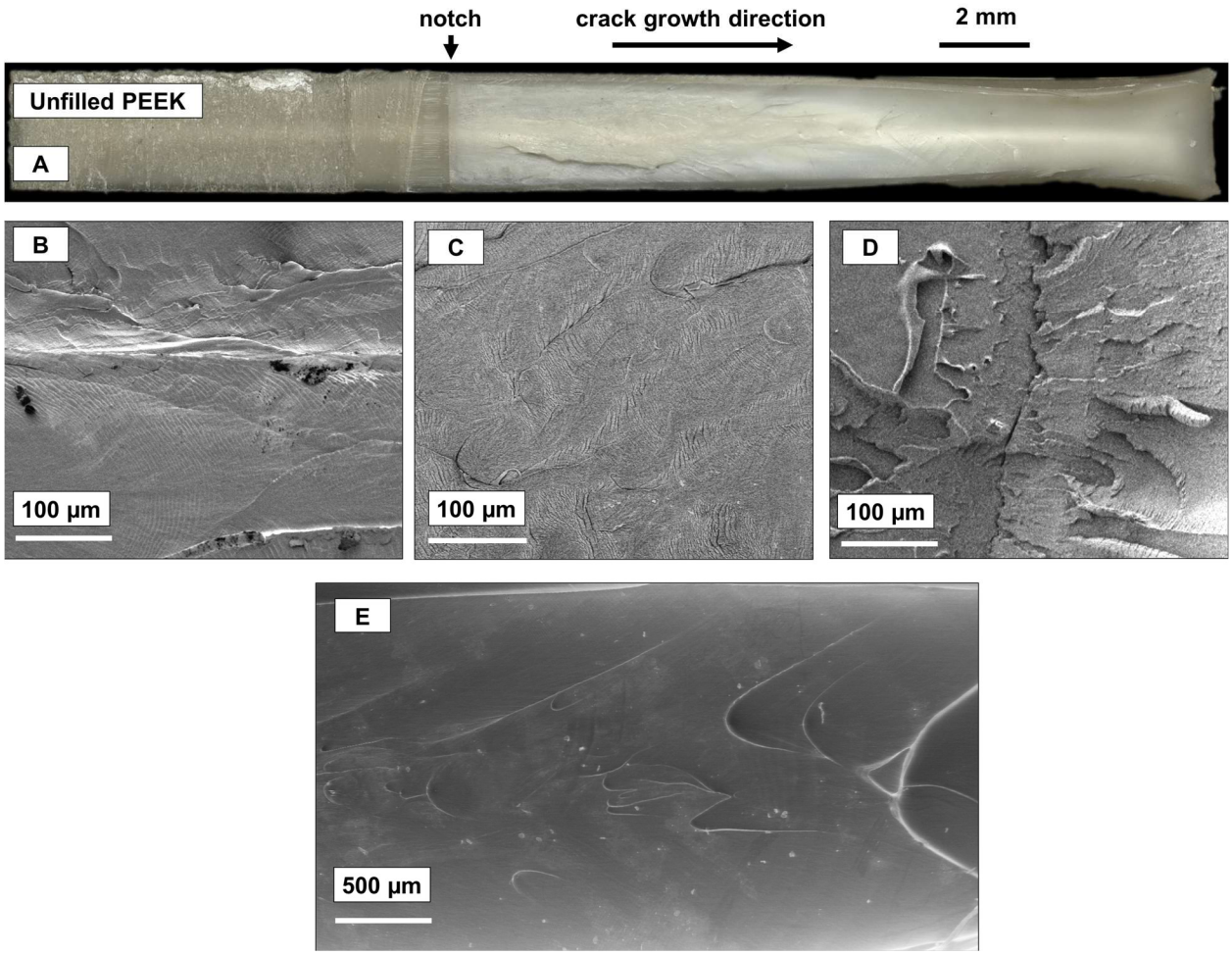

Figure 7. Images of the fracture surfaces of fatigue tested unfilled PEEK (non-heat-treated formulations). B: Early growth region. C: Mid growth region. D: Fast fracture region. E: Mid-to-late growth region.

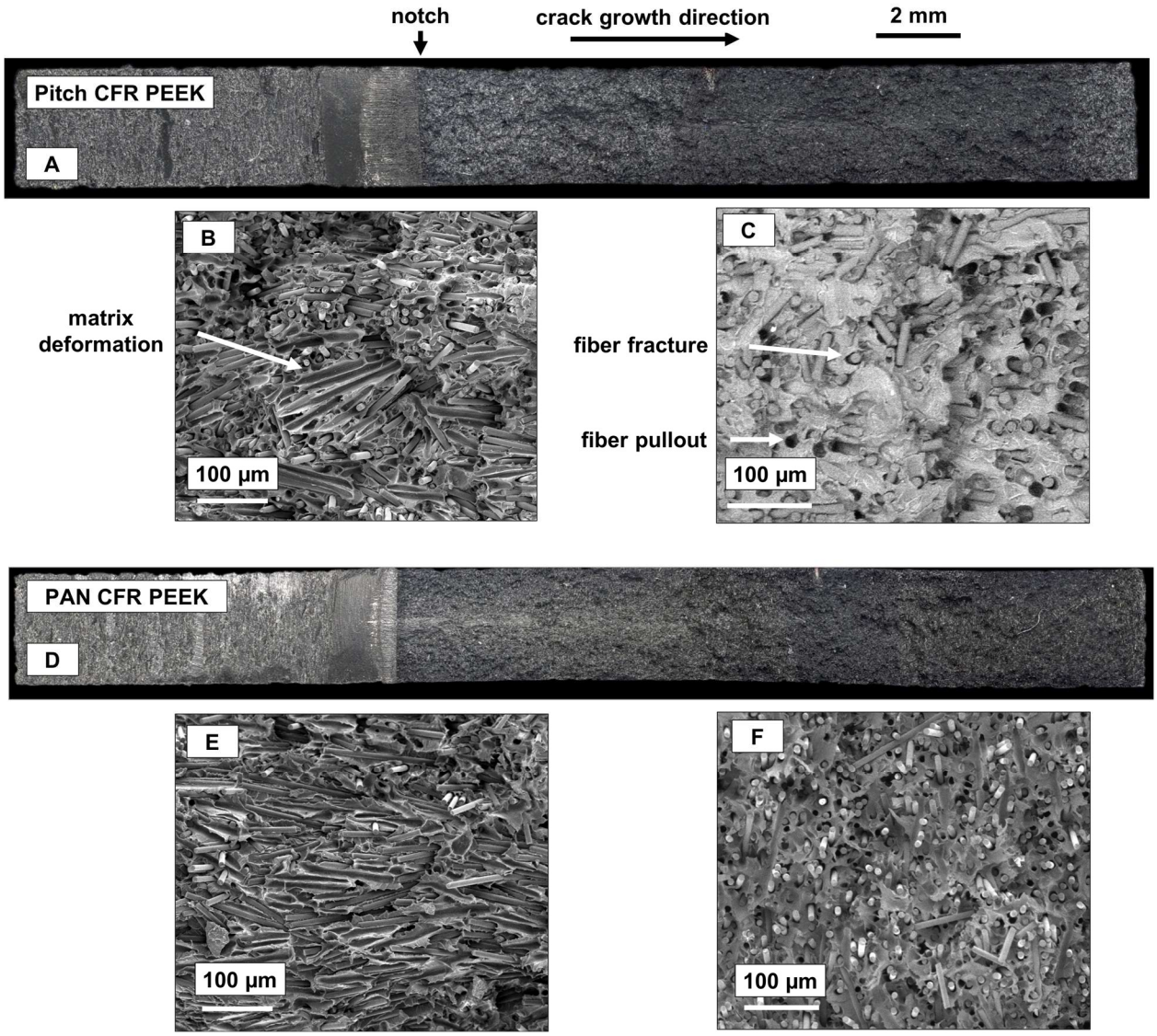

Figure 8. Images of the fracture surfaces of fatigue tested pitch (top) and PAN (bottom) CFR PEEK (non-heat-treated formulations). B and E: Early growth region. C and F: Fast fracture region.

7. Acknowledgements

The authors would like to acknowledge Limacorporate SpA for material and manufacturing support.

8. Bibliography

[1] Kurtz S. An Overview of PEEK Biomaterials. In: Kurtz S, editor. PEEK Biomaterials Handbook. 2012. p. 1–7.

[2] Kurtz S, Devine J. PEEK biomaterials in trauma, orthopedic, and spinal implants. *Biomaterials*. 2007;28(32):4845–69.

[3] Kumar S, Anderson D, Adams W. Crystallization and Morphology of Poly(aryl-ether-ether-ketone). *Polymer (Guildf)*. 1986;27:329–36.

[4] Reitman M, Jaekel D, Siskey R, et al. Morphology and crystalline architecture of polyaryletherketones. In: Kurtz S, editor. PEEK Biomaterials Handbook. 2012. p. 49–60.

[5] Green S, Schlegel J. A Polyaryletherketone Biomaterial for use in Medical Implant Applications. In: Polymers for the Medical Industry, Proceedings of a Conference held in Brussels. 2001. p. 1–7.

[6] Blundell D, Osborn B. The Morphology of Poly(aryl-ether-ether-ketone). *Polymer (Guildf)*. 1983;24:953–8.

[7] Tung C, Dynes P. Morphological characterization of polyetheretherketone-carbon fiber composites. *J Appl Polym Sci*. 1987;33:505–20.

[8] Mehmet-Alkan A, Hay J. The Crystallinity of PEEK Composites. *Polymer (Guildf)*. 1993;34(16):3529–31.

[9] Velisaris C, Seferis J. Heat Transfer Effects on the Processinge-Structure Relationships of Polyetheretherketone (PEEK) Based Composites. *Polym Eng Sci*. 1988;28(9):583–91.

[10] Ernstberger T, Buchhorn G, Heidrich G. Artifacts in spine magnetic resonance imaging due to different intervertebral test spacers. *Neuroradiology*. 2008;51:525–9.

[11] Panfili E, Pierdicca L, Salvolini L, et al. Magnetic resonance imaging (MRI) artefacts in hip prostheses: A comparison of different prosthetic compositions. *Radiol Medica*. 2014;119:113–20.

[12] Brantigan J, Steffee A. A Carbon Fiber Implant to Aid Interbody Lumbar Fusion: Two-Year Clinical Results in the First 26 Patients. *Spine (Phila Pa 1976)*. 1993;18(14):2106–17.

[13] Sastri V. High-Temperature Engineering Thermoplastics: Polysulfones, Polyimides, Polysulfides, Polyketones, Liquid Crystalline Polymers, and Fluoropolymers. In: Plastics in Medical Devices. 2nd ed. 2014. p. 173–213.

[14] Kurtz S. Applications of polyaryletheretherketone in spinal implants. In: Kurtz S, editor. PEEK Biomaterials Handbook. 2012. p. 231–51.

[15] Rotini R, Cavaciocchi M, Fabbri D, et al. Proximal Humeral Fracture Fixation: Multicenter Study with Carbon Fiber PEEK Plate. *Musculoskelet Surg*. 2015;99:1–8.

[16] Schliemann B, Hartensuer R, Koch T, et al. Treatment of Proximal Humerus Fractures with a CFR-PEEK Plate: 2-year Results of a Prospective Study and Comparison to Fixation with a Conventional Locking Plate. *J Shoulder Elb Surg*. 2015;1282–8.

[17] Akhavan S, Matthiesen M, Schulte L, et al. Clinical and histologic results related to a low-modulus composite total hip replacement stem. *J Bone Jt Surg*. 2006;88:1308–14.

[18] Glassman A. Composite femoral stem for total hip arthroplasty. *Curr Opin Orthop*. 2008;19(1):6–10.

[19] Uhthoff H, Poitras P, Backman D. Internal Plate Fixation of Fractures: Short History and Recent Developments. *J Orthop Sci*. 2006;11:118–26.

[20] Bugbee W, Culpepper W, Engh C, et al. Long-Term Clinical Consequences of Stress-Shielding After Total Hip Arthroplasty Without Cement. *J Bone Jt Surg*. 1997;79(7):1007–12.

[21] Reilly D, Burstein A. The elastic and ultimate properties of compact bone tissue. *J Biomech*. 1975;8(6).

[22] Li C, Vannabouathong C, Sprague S, et al. The use of carbon-fiber-reinforced (CFR) PEEK material in orthopedic implants: A systematic review. *Clin Med Insights Arthritis Musculoskelet Disord*. 2014;8:33–45.

[23] Wang A, Lin R, Stark C, et al. Suitability and limitations of carbon fiber reinforced PEEK composites as bearing surfaces for total joint replacements. *Wear*. 1999;225–229:724–7.

[24] Polineni V, Wang A, Essner A, et al. Characterization of Carbon Fiber-Reinforced PEEK Composite for use as a Bearing Material in Total Hip Replacements. *ASTM Int*. 1998;266–73.

[25] Regis M, Lanzutti A, Bracco P, et al. Wear behavior of medical grade PEEK and CFR PEEK under dry and bovine serum conditions. *Wear*. 2018;408–409(May):86–95.

[26] Invibio. PEEK-OPTIMA Wear Performance: Typical Material Properties [Internet]. 2013 [cited 2016 May 2]. Available from: https://invibio.com/ortho/materials/peek-optima-wear-performance

[27] Flock J, Friedrich K, Yuan Q. On the friction and wear behaviour of PAN-and pitch-carbon fiber reinforced PEEK composites. *Wear*. 1999;225–229:304–11.

[28] Huang X. Fabrication and properties of carbon fibers. *Materials (Basel)*. 2009;2(4):2369–403.

[29] Regis M, Fusi S, Favaloro R, et al. CFR PEEK composites for orthopaedic applications. In: 9th International Conference on Composite Science and Technology. 2013.

[30] Yuan Q, Bateman S, Friedrich K. Thermal and mechanical properties of PAN- and pitch-based carbon fiber reinforced PEEK composites. *J Thermoplast Compos Mater*. 2008;21(4):323–36.

[31] Sardar Z, Jarzem P. Failure of a Carbon Fiber-Reinforced Polymer Implant Used for Transforaminal Lumbar Interbody Fusion. *Glob Spine J*. 2013;3(4):253–6.

[32] Tullberg T. Failure of a Carbon Fiber Implant. A Case Report. *Spine (Phila Pa 1976)*. 1998;23(16):1804–6.

[33] Ansari F, Chang J, Huddleston J, et al. Fractography and oxidative analysis of gamma inert sterilized posterior-stabilized tibial insert post fractures: Report of two cases. *Knee*. 2013;20(6):609–13.

[34] Tower A, Currier J, Currier B, et al. Rim Cracking of the Cross-Linked After Total Hip Arthroplasty. *J Bone Jt Surg*. 2007;2212–7.

[35] Bonnheim N, Gramling H, Ries M, et al. Fatigue fracture of a cemented Omnifit CoCr femoral stem: implant and failure analysis. *Arthroplast Today*. 2017;3:234–8.

[36] Saib K, Isaac D, Evans W. Effects of processing variables on fatigue in molded PEEK and its short fiber composites. *Mater Manuf Process*. 1994;9(5):829–50.

[37] Saib K, Evans W, Isaac D. The role of microstructure during fatigue crack growth in poly (aryl ether ether ketone) (PEEK). *Polymer (Guildf)*. 1993;34(15):3198–203.

[38] Brillhart M, Botsis J. Fatigue crack growth analysis in PEEK. *Int J Fatigue*. 1994;16:134–40.
[39] Brillhart M, Botsis J. Fatigue fracture behavior of PEEK: 2. Effects of thickness and temperature. *Polymer (Guildf)*. 1992;33(24):5225–32.
[40] Brillhart M, Gregory B, Botsis J. Fatigue fracture behavior of PEEK: 1. Effects of load level. *Polymer (Guildf)*. 1991;32(9):1605–11.
[41] Karger-Kocsis J, Walter R, Friedrich K. Annealing effects on the fatigue crack propagation of injection-moulded PEEK and its short fibre composites. *J Polym Eng*. 1988;8(3–4):221–53.
[42] Chu J, Schultz J. The influence of microstructure on the failure behaviour of PEEK. *J Mater Sci*. 1990;25:3746–52.
[43] Friedrich K, Walter R, Voss H, et al. Effect of short fibre reinforcement on the fatigue crack propogation and fracture of PEEK-matrix composites. *Composites*. 1986;17(3):205–16.
[44] Evans W, Isaac D, Saib K. The effect of short carbon fibre reinforcement on fatigue crack growth in PEEK. *Composites*. 1996;27A:547–54.
[45] Regis M, Zanetti M, Pressacco M, et al. Opposite role of different carbon fiber reinforcements on the non-isothermal crystallization behavior of poly(etheretherketone). *Mater Chem Phys*. Elsevier B.V; 2016;179:223–31.
[46] Regis M, Bellare A, Pascolini T, et al. Characterization of thermally annealed PEEK and CFR-PEEK composites. *Polym Degrad Stab*. 2017;136:121–30.
[47] Maksimov R, Kubat J. Time and temperature dependent deformation of poly(ether ether ketone) (PEEK). *Mech Compos Mater*. 1997;33(6):517–25.
[48] Ansari F. The Interplay of Design and Materials in Orthopedics: Evaluating the Impact of Notch Geometry on Fatigue Failure of UHMWPE Joint Replacements. Dissertation, UC Berkeley. 2015.
[49] Invibio. PEEK-OPTIMA Natural: Typical Material Properties [Internet]. 2013 [cited 2016 Apr 18]. Available from: https://invibio.com/library?id=%7B9ec81b92-8ab8-40da-af8f-6c3bf002aa84%7D
[50] Invibio. PEEK-OPTIMA Reinforced: Mechanical Properties, Physical Properties and Biocompatibility [Internet]. 2014 [cited 2016 Apr 18]. Available from: https://invibio.com/library?id=%7B4957faed-3d7d-466b-bed0-f8dfcf1a6e5a%7D
[51] Lafdi K, Wright M. Carbon fibers. In: Peters S, editor. Handbook of Composites. London: Chapman & Hall; 1998. p. 169–201.